

Article

An Integrated Method for Identifying Present Status and Risk of Drought in Bangladesh

Md. Latifur R. Sarker ^{1,*}, Nichol Janet ², Siti A. Mansor ³, Baharin Bin Ahmad ³, Shamsuddin Shahid ⁴ , Eun-Sung Chung ⁵ , Jeffrey S. Reid ⁶ and Eko Siswanto ⁷ 

¹ Department of Geography and Environmental Studies, University of Rajshahi, Rajshahi, Rajshahi 6205, Bangladesh

² Department of Geography, School of Global Studies, University of Sussex, Brighton BN19RH, UK; janet.nichol@connect.polyu.hk

³ Department of Geoinformation, Faculty of Built Environment & Surveying, Universiti Teknologi Malaysia, Johor Bahru 81310, Malaysia; echizen@gmail.com (S.A.M.); baharinahmad@utm.my (B.B.A.)

⁴ Department of Water and Environmental Engineering, School of Civil Engineering, Faculty of Engineering, Universiti Teknologi Malaysia, Johor Bahru 81310, Malaysia; sshahid@utm.my

⁵ Dept of Civil Engineering, Seoul National University of Science & Technology, 232 Gongneung-ro, Nowon-gu, Seoul 01811, Korea; eschung@seoultech.ac.kr

⁶ Marine Meteorology Division, Naval Research Laboratory, Monterey, CA 93943, USA; jeffrey.reid@nrlmry.navy.mil

⁷ Research and Development Center for Global Change (RCGC), Japan Agency for Marine-Earth Science and Technology (JAMSTEC) 3173-25, Showa-machi, Kanazawa-ku, Yokohama, Kanagawa 236-0001, Japan; ekosiswanto@jamstec.go.jp

* Correspondence: lrsarker@ru.ac.bd

Received: 7 June 2020; Accepted: 17 August 2020; Published: 20 August 2020



Abstract: The occurrence and severity of agricultural droughts may not be dependent upon climatic variables alone. Rather increasingly, drought is affected by human interventions such as irrigation. Anthropogenic activity has introduced uncertainty in the assessment of current drought and future drought risk in many parts of the world; neither climatic nor remote sensing data alone are able to assess drought conditions effectively. In response, we present a simple approach to assess drought by combining a remote sensing-based drought index, the Temperature Vegetation Dryness Index (TVDI), climate data (i.e., rainfall and temperature), and field observations to evaluate recent drought conditions in northwestern Bangladesh (NWB). Applying this approach, we gained five insights: (i) the TVDI successfully indicated the drought conditions of NWB and agrees with field observations, (ii) the integrated use of TVDI and climate data (such as rainfall and temperature) provides the best understanding of the difference between meteorological drought and droughts resulting from surface moisture conditions, (iii) the TVDI results agree with rainfall data ($r^2 = 0.40$ in March and $r^2 = 0.46$ in April) in a part of the study area (NWB) where irrigation is not available, (iv) the TVDI can be used along with climate data to predict the potential risk of drought, and (v) while meteorological drought exists due to low rainfall and high temperature in this NWB in pre-monsoon season, because of widespread irrigation practices, meteorological drought is unable to trigger agricultural drought over most parts of the study area. The findings imply that there is a potential risk of drought in NWB, since any disruption of irrigation water supply could trigger a severe agricultural drought over the whole region. This is similar to what is currently observed over a small part of NWB.

Keywords: remote sensing; TVDI; drought; food production; Bangladesh

1. Introduction

Drought is recognized as a complex natural disaster that has severe effects on wildlife, agriculture, and the economy [1–3]. The number of people affected by drought is greater than from any other class of natural disaster [2,4]. In recent years, the frequency and severity of droughts are increasing due to several factors, including climate change. Indeed, there have been many large-scale droughts affecting sizable areas of Europe, Africa, Asia, Australia, South America, Central America, and North America that can be linked to significant economic losses, food shortages, and in some cases, starvation for millions of people [5–7].

Agriculture is always the first sector to be affected by the onset of drought [8–10]. The adverse effects of drought are normally increased if drought occurs in an agrarian and densely populated region, such as South Asia, where millions of people are directly or indirectly dependent on diverse agricultural activities [11]. However, the severity of drought in some parts of South Asia such as in Bangladesh has been extensively reduced by intensive irrigation, using easily available but slowly declining underground water for the cultivation of high yield variety (HYV) boro rice [12].

Massive irrigation practices during the hot pre-monsoon season has created a complex scenario: (i) meteorological drought, which exists mainly due to high temperature and low rainfall, (ii) agricultural drought, which may or may not occur depending on the availability of irrigation, and (iii) a future threat to irrigation practices due to the regular depletion of underground water. This situation urgently requires detailed investigation of recent drought scenarios to minimize the potential risk of agricultural drought and its consequences for food security. However, a clear quantification of drought is not easy to accomplish in complex environmental settings that have evolved over decades through the integration of climate variables (temperature and rainfall) with human activities (i.e., irrigation and groundwater extraction) [13,14].

Significant efforts have been made to develop drought indices. Indeed, hundreds of drought indices, broadly based on meteorological and satellite data, have been developed [15,16]. The use of meteorological data-based drought indices, such as the Standardized Precipitation Index (SPI [17]) and the Palmer Drought Severity Index (PDSI [18]) are common in the literature [15]. Similarly, the use of satellite-derived indices such as the Normalized Difference Vegetation Index (NDVI) [19], the Vegetation Condition Index (VCI) [20], the Temperature Condition Index (TCI) [20], the Vegetation Health Index (VHI) [20], and the Temperature Vegetation Dryness Index (TVDI) [21] for the detection of drought have been well documented [21–23].

Despite the apparent successful use of drought indices, there are reports that indices based on meteorological data or remote sensing data alone have limitations for the characterization of drought [15]. This is especially true when anthropogenic activity modifies the surface conditions. Thus, in complex environmental settings, both types of drought index are limited: (i) meteorological data-based indices are unable to address the surface moisture contributed by anthropogenic activities and (ii) satellite-based drought indices are largely able to address the surface moisture conditions but unable to recognize the potential of climatological drought. Both factors are vital for understanding future drought risk.

Consequently, numerous studies have attempted to (i) develop new models [24–27], (ii) use multiple indices and ancillary data [28–30], (iii) combine meteorological indices and remote sensing indices [31], and (iv) use multi-sensor data [32–34] in an endeavor to quantify the irregularities in reporting of drought intensity and spatial–temporal extent. However, none of these studies have been able to detect drought or foresee future drought, which requires distinguishing between moisture sources (i.e., rainfall or anthropogenic sources). For example, the SPI is based on meteorological data, comparing rainfall at a given location with historic rainfall records. The TDVI combines optical and thermal wavebands of satellite images to estimate the degree of moisture stress in vegetation canopies. However, the drought stress detected by either index cannot inform the cause of the drought or the risk of future drought.

Given the challenge of applying single source drought indices to a multi-dimensional problem, this study develops an integrated method that quantifies the present drought status and allows an examination of the potential risk of drought by integrating remote sensing-based drought indices, climate

data (i.e., rainfall and temperature), and field observations. This paper considers several important requirements: (i) the need for an effective drought assessment technique for complex drought settings, where drought detection is difficult using either remote sensing or climate data-based drought indices alone, (ii) the importance of future agricultural drought risk assessment for this densely populated region, to ensure food security, and (iii) to explore the possibility of relating satellite-driven drought measurement with climate variables and field investigations.

2. Study Area and Selection of Data and Drought Index

2.1. Study Area

Bangladesh is one of the most drought-prone countries in the world [35], although massive irrigation practices have reduced the pre-monsoon drought intensity in many areas. The area of northwestern Bangladesh (NWB, Figure 1), having higher rainfall variability and drier climate [36], is the most drought-affected part of the country [37,38] and was selected for this study.

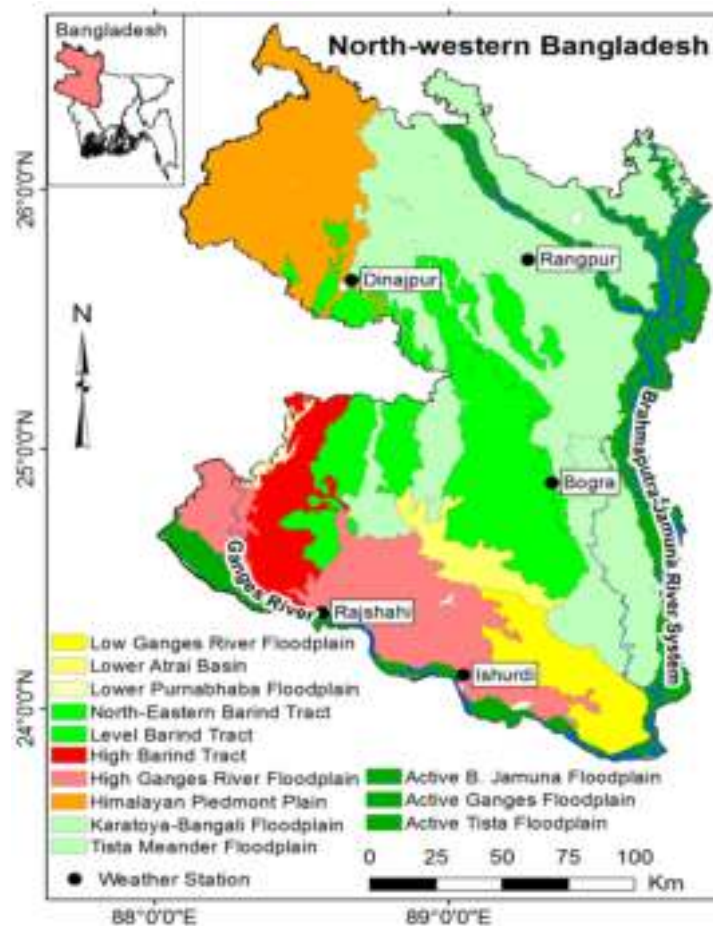


Figure 1. Study area with several major and minor physiographic units.

Geomorphologically, NWB is divided into four major physiographic units: (i) Barind Tract (High Barind Tract (HBT), level Barind Tract, North-Eastern Barind Tract), (ii) Himalayan piedmont plains, (iii) alluvial floodplains (Karatoya-Bangali floodplain, Tista Meander floodplain, low Ganges River floodplain (GRFP), high GRFP, lower Punarbhaba floodplain, and lower Atrai basin), and (iv) active river floodplains (Brahmaputra-Jamuna floodplain, Ganges floodplain, and Tista floodplain) [39]. These major and minor physiographic divisions fundamentally determine the intensity of drought, as well as cropping patterns and the ability to cultivate irrigated HYV boro rice in this region.

Temperatures in the region range from 25 to 40 °C in the hottest pre-monsoon season and from 8 to 25 °C in the coolest winter season. Almost all rainfall occurs during May to October, with less than 6% occurring during the dry season (January to April) [40]. Cultivation takes place all year round across most areas of Bangladesh, with double/triple crop planting necessary to support the farming economy. Rice is the main crop, with the HYV boro rice being cultivated during the dry season and representing almost 88% of total cultivated croplands in this season [41,42]. Due to the lack of any alternative source of water for boro rice, groundwater is the only major source of irrigation water in this region [40].

2.2. Selection of Data

Cultivation in Bangladesh takes place at all times of year, but the dry season is very important for rice cultivation. Therefore, this study investigated agricultural drought conditions in terms of moisture availability during the pre-monsoon dry season (January through April) from 2001 to 2014. Since the satellite-based TVDI was used for this study, the main data required were the (i) Normalized Difference Vegetation Index (NDVI) and (ii) Land Surface Temperature (LST). Considering suitable spatial and temporal resolution, this study used data that derived from the Moderate Resolution Imaging Spectroradiometer (MODIS) sensor. Two MODIS products, namely monthly-NDVI (MOD13A3, collection 6) and daily-LST (MOD11A1, collection 6) with spatial resolutions of 1 km were used.

In addition to satellite data, climate data (i.e., temperature and rainfall) and field observations were used to support and explain the results. Daily long-term rainfall and temperature data from five meteorological stations (Figure 1) were collected from the Bangladesh Meteorological Department (BMD). From the daily data, we have calculated the monthly average of temperature and rainfall for all the four months (i.e., January, February, March, and April). Field observations, covering a wide range of physiographic and moisture conditions, were collected from the second week of March to the second week of April in 2017. A purposive sampling strategy was adopted, and several sites were visited to cover the wide range of physiographic and TVDI variations. During the field visit, necessary pictures of all the selected sites were taken by a high-resolution camera, and the location of all the sites was determined by GPS. Several pictures were taken for each site during the field visits.

2.3. Selection of Drought Index

A number of satellite-based drought indices have been developed, which commonly combine the NDVI and LST for drought detection [20,43,44]. However, there are numerous limitations for these two indices: (i) the time lag between the occurrence of a drought and changes in the NDVI, which limits the applicability of NDVI-based methods for real time monitoring of drought [45], and (ii) when the ground is not completely covered by vegetation, the higher soil background temperature severely affects the estimation if only temperature is considered [46]. Therefore, the relationship between LST and NDVI has been investigated by several authors, and the LST-NDVI spectral space has come into widespread use for soil moisture/vegetation-related applications [45,47,48].

Based on the LST-NDVI triangle space (Figure 2), a few drought indices have been developed and used for drought monitoring. A number of studies have successfully employed the TVDI [21], which is an LST-NDVI space-based drought index, for monitoring vegetation stress, surface moisture conditions, and drought [30,49,50]. As the TVDI is computationally simple and able to effectively combine LST and NDVI for determining drought in different geographical regions [22,51], it was selected for this study.

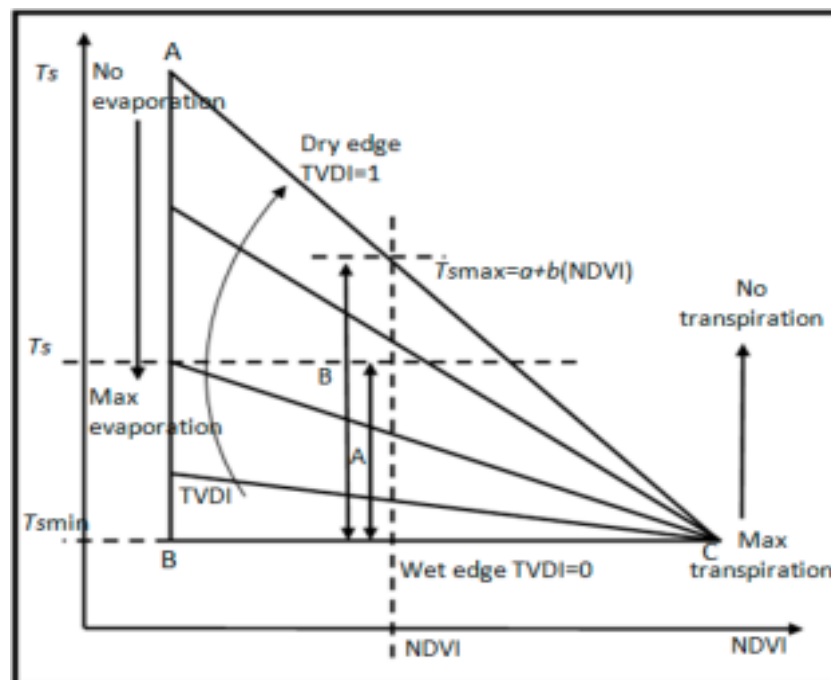


Figure 2. Simplified normalized difference vegetation index–land surface temperature (NDVI–LST) space [21]. A represents maximum dryness, B represents maximum wetness, and C represents maximum transpiration. The TVDI for a pixel (NDVI/LST) can be estimated as the position between lines A and B.

3. Method

In this study, we integrated the results of the TVDI, climate data (i.e., rainfall and temperature), and field observations for detecting present drought conditions and future drought risk. For TVDI, we followed the general methodology [21,22] for the processing of two kinds of MODIS satellite, i.e., NDVI and LST. Thus, the overall data processing method of this study comprises four steps: (i) pre-processing, (ii) calculation of TVDI, (iii) integration of the TVDI results with climate variables (i.e., temperature and rainfall), and (iv) comparison of the TVDI results with field observations. These are described in the following subsections.

3.1. Pre-Processing

All of the downloaded NDVI and LST images were pre-processed as follows: (i) the necessary data (i.e., NDVI, LST, and quality assessment files) were extracted and re-projected using the MODIS Conversion Toolkit, using the Universal Transverse Mercator (UTM) projection and World Geodetic System (WGS) 84 datum, (ii) complete coverage of the study area was obtained by mosaicking two tiles, followed by sub-setting to include the study area only, (iii) a temporal averaging process was carried out to produce monthly LST from the daily LST product (MOD11A1, collection 6), since we have used monthly NDVI (MOD13A3) for generating the TVDI, and (iv) LST values were converted from Kelvin to Celsius.

3.2. Calculation of TVDI

A conceptual NDVI–LST space, with LST plotted as a function of NDVI, is presented in Figure 2. Based on the NDVI–LST space empirical relation, a simplified water stress/dryness index (TVDI) was suggested by [21]. In this approach, the “wet edge” is modeled as a horizontal line (i.e., parallel to

the NDVI axis) as opposed to a sloping wet edge in the trapezoid approach, and the “dry edge” is modeled as a linear fit to NDVI [49,51]. According to [21], the TVDI can be defined simply as:

$$TVDI = \frac{LST - LST_{min}}{a + b(NDVI) - LST_{min}}. \quad (1)$$

In Equation (1), LST is the observed surface temperature at the given pixel, NDVI is the observed normalized difference vegetation index, and a and b are the intercept and slope of the dry edge, respectively (the upper straight line in the triangle) (Figure 2) calculated from NDVI–LST space regression with small intervals of NDVI ($LST_{max} = a1 + b1*NDVI$), where LSTmax is the maximum surface temperature observation for a given NDVI value. The lower horizontal line of the triangle represents the wet edge ($LST_{min} = a2 + b2*NDVI$) (Figure 2), which can be calculated by averaging a group of points in the lower limits of the LST–NDVI scatterplots [21]. Both the dry edge (LSTmax) and wet edge (LSTmin) are determined by linear regression analysis.

For this calculation, we first filtered out water pixels from NDVI and any unwanted LST values from the pre-processed MODIS NDVI and LST data. Then, we sliced the NDVI values into 100 intervals of 0.01 to obtain LST values for each NDVI interval. We applied least-squares regression fitting to extract the maximum LST value and the minimum LST value of the NDVI interval in steps of 0.01 from the LST–NDVI trapezoid to obtain the fitting equations for the dry edge ($LST_{max} = a1 + b1*NDVI$) and the wet edge ($LST_{min} = a2 + b2*NDVI$). Once these two edges were obtained, we produced the TVDI for each month using Equation (1).

The TVDI was calculated for January through April from 2001 to 2014 for several reasons: (i) January is the coldest and driest month while April is the hottest, (ii) rainfall is very low and temperatures rise quickly in later part of this period, (iii) the soil moisture deficit is ubiquitous, (iv) many severe drought events have occurred during the latter part of this period, and (v) High Yielding Variety (HYV) boro rice, which is essential to the economy, and which requires a plentiful moisture supply, is cultivated during these months.

The results of the TVDI and its spatial and temporal variation are presented in two ways: (i) by the simple stretching of the TVDI between 0 and 1 (Figure 3A and Figure S1A) and (ii) by classifying the TVDI into five categories [22] (Figure 3B and Figure S1B). The five TVDI categories are wet (0–0.2), normal (0.2–0.4), slight drought (0.4–0.6), moderate drought (0.6–0.7), and severe drought (0.7–1). However, slight changes in the last two categories of the TVDI were made. These included using the TVDI with an upper limit of 0.7 for moderate drought instead of 0.8 and adjusting the TVDI range for the last category, taking into account the effect of massive irrigation practices.

3.3. Integration of TVDI Results with Climate Variables

Integration of the TVDI results with the climate variables temperature and rainfall was performed as follows. First, the study area was divided into two groups based on the classified TVDI values i.e., (i) $TVDI < 0.07$, and (ii) $TVDI > 0.70$, where $TVDI < 0.07$ indicates very low to moderate drought condition and $TVDI > 0.70$ indicates high to severe drought condition. Secondly, the percentage area in each group was calculated for all four months (i.e., January, February, March, and April) over the whole period. Finally, besides graphical presentation, a statistical relationship was determined by estimating the correlation coefficient (r) between the area of each TVDI group and the climate variables for each month and subsequently for each year over the period.

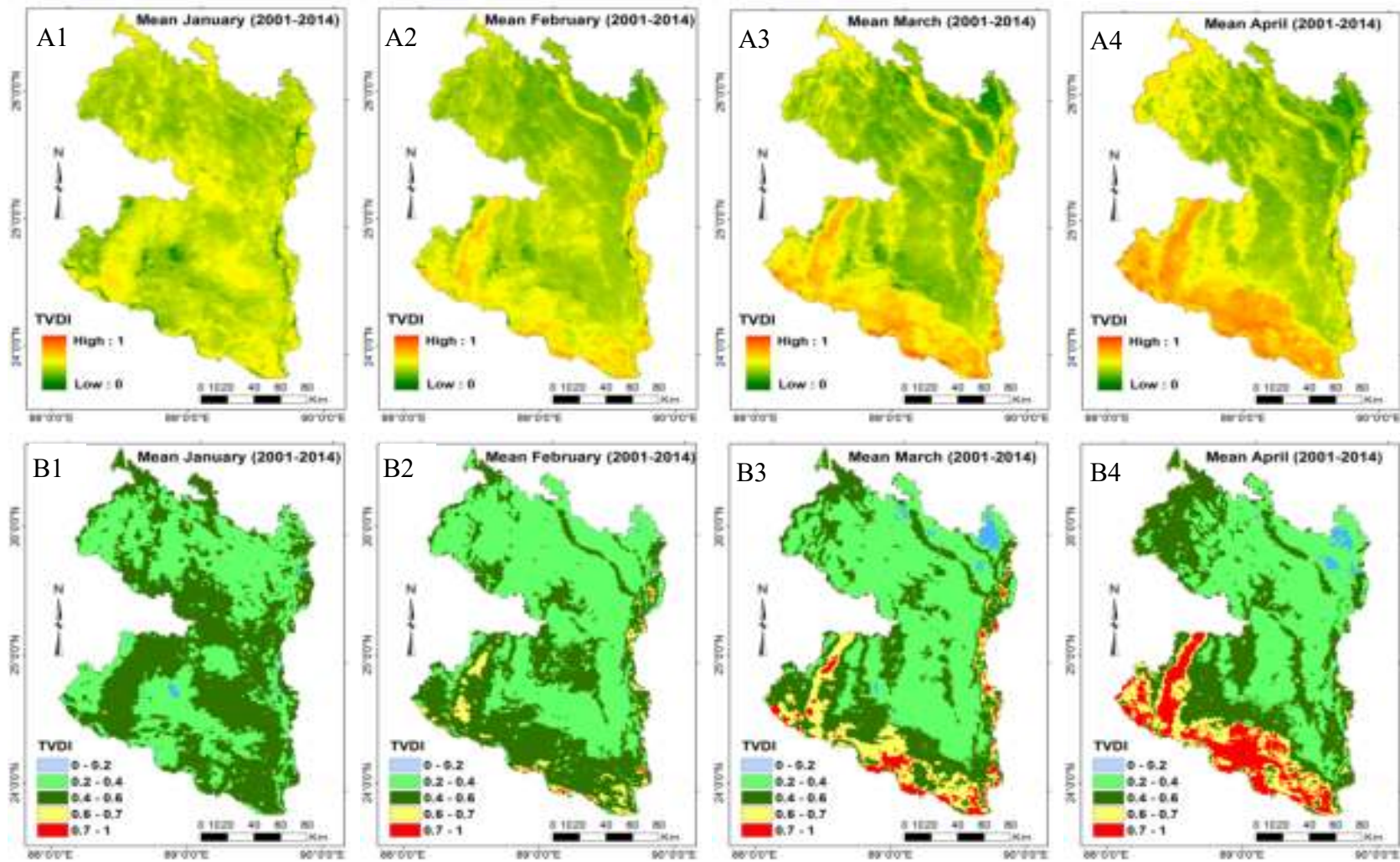


Figure 3. Monthly mean spatial distribution of the Temperature Vegetation Dryness Index (TVDI), for January, February, March, and April over 14 years (2001–2014) (3A): stretched and (3B): classified.

3.4. Comparison of TVDI Results with Field Observations

The collected field observations were examined, and these qualitative data were used for two purposes i.e., (i) to understand the relationship between the TVDI results and field conditions and (ii) to solve two opposite arguments: why in large parts of the study area, the TVDI results disagree with climate data (i.e., rainfall and temperature), and why in small parts of the study area, the TVDI results agree with climate data. All the field observations are presented as figures, and their characteristics explained with respect to the TVDI results in Section 4.3).

4. Results

Results are presented in three groups: (i) assessment of drought using the TVDI, (ii) integration of TVDI results with climate variables, and (iii) comparison of TVDI results with field observations.

4.1. Assessment of Drought using TVDI

Fourteen years (2001–2014) of mapped monthly (i.e., January, February, March, and April) mean TVDI (Figure 3) and likewise 14 years of individual months (S1A and S1B) indicate that the TVDI varies spatially and temporally within the pre-monsoon 4-month period (i.e., 4 months within a single year) as well as for each month among different years. In a single period/year (e.g., January–April 2001), a very low to moderate drought condition ($\text{TVDI} < 0.70$) was observed almost throughout the study area in the months of January and February. Moreover, a similar drought situation ($\text{TVDI} < 0.7$) was observed in the months of March and April, but with higher TVDI areas ($\text{TVDI} > 0.7$), which indicates severe drought problems were observed, mostly in the HBT as well as along the GRFP, both in the south of the study area (Figure 1). The variation of the TVDI over the January to April period of all other years is notably similar, where the TVDI is mostly low in January and increases gradually, becoming highest in the hottest months of March and April and indicating severe drought over a small part of the study area in northwestern Bangladesh.

The inter-annual variation of the TVDI for the single month of January was low (e.g., January 2001 to January 2014) (Column 1 of Figure S1A,B), indicating no major change in the spatial distribution of the TVDI over the 14-year period. The TVDI for January was nearly always low over the 14-year period, indicating that no severe drought-prone areas were observed. The one exception was 2002, when a few areas were found to be suffering severe drought ($\text{TVDI} > 0.7$). A stable pattern of inter-annual variation of the TVDI was also observed for the month of February (Column 2 of Figure S1A,B), although more areas with higher TVDI values were noticed compared to January. Similar to January and February, the inter-annual spatial variation of the TVDI in March and April during this 14-year period was not also noteworthy. Generally, the high TVDI representing severe drought was observed in April, over approximately 15% of NWB, notably in the southern part of the study area, throughout the 14-year period, although the TVDI for most of NWB was still < 0.70 ; i.e., it was not severe (Columns 3 and 4 of Figure S1A,B).

The simple finding from the above results is that NWB did not suffer much from severe drought during the four selected months (i.e., January through April) over the 14-year period. Very few severely drought-prone areas ($\text{TVDI} > 0.7$) were detected in January and February over the period; therefore, these two months can be considered as less susceptible to drought hazard. Considering the large areas with slight to moderate drought ($\text{TVDI} > 0.40$ to < 0.70), March and April can also be considered primarily free from drought risk as well. However, small parts of NWB (mostly in the south and south-western part) were affected by severe drought ($\text{TVDI} > 0.70$) throughout the 14-year period, indicating that these two months are not completely free from drought risk.

The outcomes obtained using the TVDI are not in agreement with the findings of several previous drought studies based on meteorological data [52,53]. These studies indicate the northwestern part of Bangladesh as the most drought-prone area in the country and also that droughts during the pre-monsoon summer (March–April) are severe due to high temperature and low rainfall. Therefore,

in this study, an effort has been made to integrate the TVDI results with climate data (i.e., temperature and rainfall) in order to understand the anomalies between this and previous studies [52,53], as well as to put the TVDI outcomes observed in context of climate data.

4.2. TVDI Results with Temperature and Rainfall

To integrate the TVDI results and climate data, we first categorized the TVDI results into two groups: (i) TVDI < 0.07 (very low to moderate drought conditions (hereafter lowTVDI)) and (ii) TVDI > 0.70 (severe drought conditions (hereafter highTVDI)).

4.2.1. Integration of LowTVDI Area with Temperature and Rainfall

Figure 4 shows temperature and rainfall in the areas of lowTVDI (TVDI < 0.7 representing low to moderate drought) in all years. In these areas, temperatures increase rapidly from January to February and February to March, and at a slower pace from March until the peak in April (Figure 4A). This pattern of temperature increase is consistent over the 14-year period with slight anomalies in a few years such as 2001, 2002, 2011, and 2012 (Figure 4A). Similar to temperature, rainfall also increases from January and reaches its peak in April, although variation in rainfall from year to year is evident (Figure 4A). The lowTVDI areas appear to be greatest in January (99.99% in 2005) and gradually decrease during the season. The least area of lowTVDI occurs in April (79.50% in 2001), although some variation in this trend is noticeable, especially for April in 2002, 2003, 2006, and 2011 (Figure 4A).

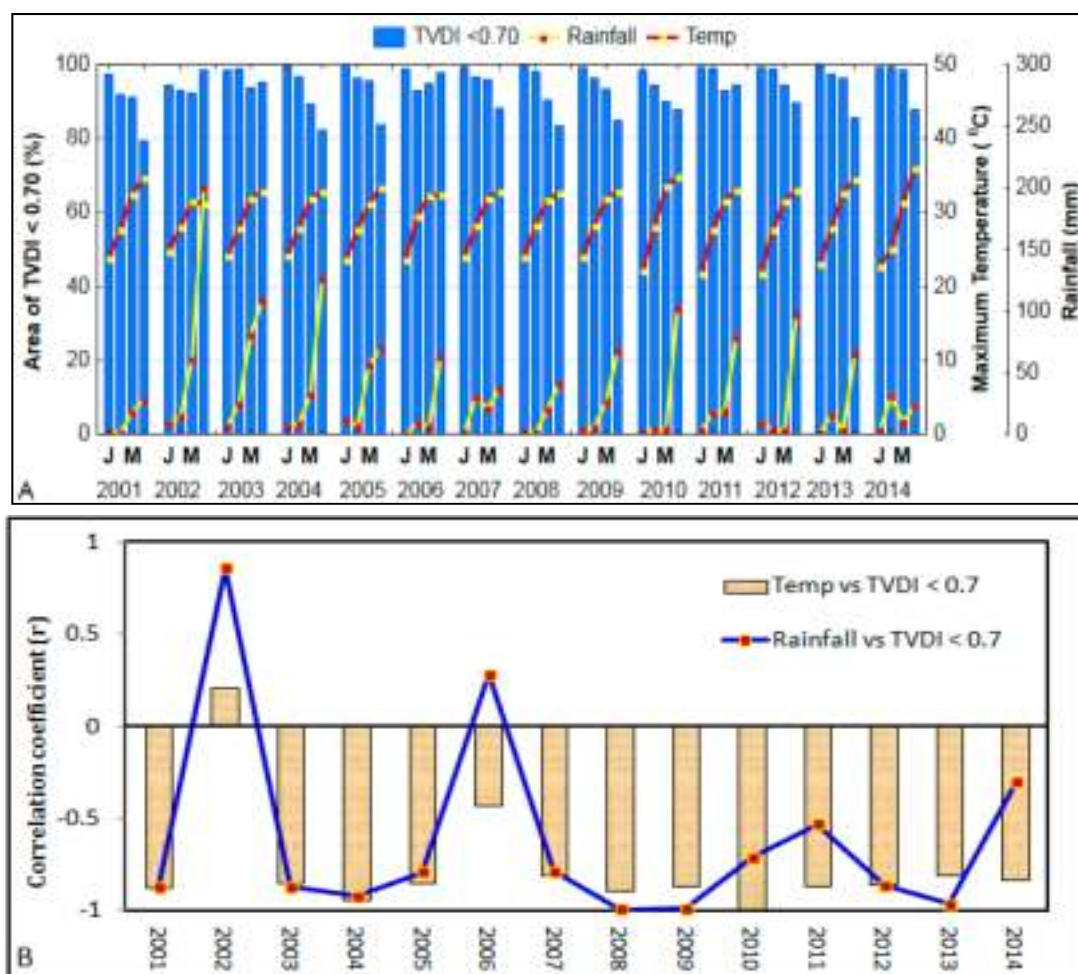


Figure 4. Relationship between lowTVDI and temperature and rainfall. (A) is the integrated display of lowTVDI area, rainfall and temperature where J indicates January and M indicates March; (B) is the correlation between area of lowTVDI and temperature, as well as between lowTVDI and rainfall.

In general, strong negative correlation was observed between the area of lowTVDI and temperature, as well as between lowTVDI and rainfall, except in the years 2002 and 2006 (Figure 4B). The negative correlation found is expected, as high temperature increases evaporation, resulting in soil moisture deficit. Notably, in spite of the strong negative relationship between temperature and the TVDI, approximately 80% of the study area is still unaffected by drought (indicated by lowTVDI), even in March and April, when the average temperature is above 32 °C (Figure 4A). This situation contradicts expected scenarios and suggests three possibilities: (i) soil moisture is available from the adequate rainfall or stored soil moisture from previous months, (ii) there is an additional supply of water apart from rainfall, and (iii) the TVDI results are not representative of climate data.

The rainfall during the period increases between January and April (Figure 4A) but the extent of lowTVDI areas (not drought-affected) does not increase; therefore, we obtained a negative correlation between lowTVDI areas and rainfall (Figure 4B). A negative correlation between lowTVDI and rainfall is not expected since high rainfall increases soil moisture, resulting in lowTVDI. However, the impact of rainfall on the lowTVDI area is not observable, since the rainfall is very low over the whole dry season (January to April) period (Figure 4A). Moreover, the possibility of moisture supply from the rainfall of the previous months, November and December, is also low, since the average rainfall in November and December is less than 10 mm/month. Therefore, it is understood from the climate data and previous studies that soil moisture in these lowTVDI areas (mostly planted to HYV boro rice) has been supplied by intensive groundwater-based irrigation systems [41,42] to meet the irrigation requirements of an average of 8.8 mm/day [40]. A report [54] indicated that the contribution of groundwater to HYV boro rice cultivation increased from 41% in 1982/83 to 85% in 2009/2010. This explains the observed disagreement between lowTVDI area and rainfall data.

4.2.2. Integration of the HighTVDI Area with Temperature and Rainfall

It is worthwhile to note that highTVDI areas were consistently observed over only a minor portion of NWB in the south and southwest (Figure 3, Figure S1A,B). These sites belong to the High Barind Tract and High Ganges River Floodplain (Figure 1) where irrigation facilities are mostly unavailable.

It is obvious that highTVDI areas are negligible or absent in January and increase gradually, reaching the highest percentage (maximum of 20%) in April (Figure 5A). The increase in highTVDI area with respect to time (month) is positively correlated with both temperature and rainfall (Figure 5B). The positive agreement between highTVDI area and temperature is expected, but that with rainfall is not.

The positive agreement between highTVDI and rainfall (Figure 5B) may have occurred due to the averaging of rainfall data from all 5 weather stations across NWB (Figure 1), of which only two (i.e., Rajshahi and Ishwardi, Figure 1) are located near the highTVDI areas. Based on rainfall data from these two stations, results for the months of March using 12 years of data (Figure 6A) and April using 13 years of data (Figure 6B) showed a negative correlation ($R = -0.63$ for March and $R = -0.68$ for April) between highTVDI area and rainfall.

The negative agreement between the highTVDI area and rainfall, and the positive correlation between highTVDI and temperature, demonstrated that both of these climate variables have a direct impact on the drought situation in the part of NWB where highTVDI values were found continuously over the period. At this point, remote sensing drought index results (i.e., TVDI results) are in agreement with the variation of rainfall and temperature.

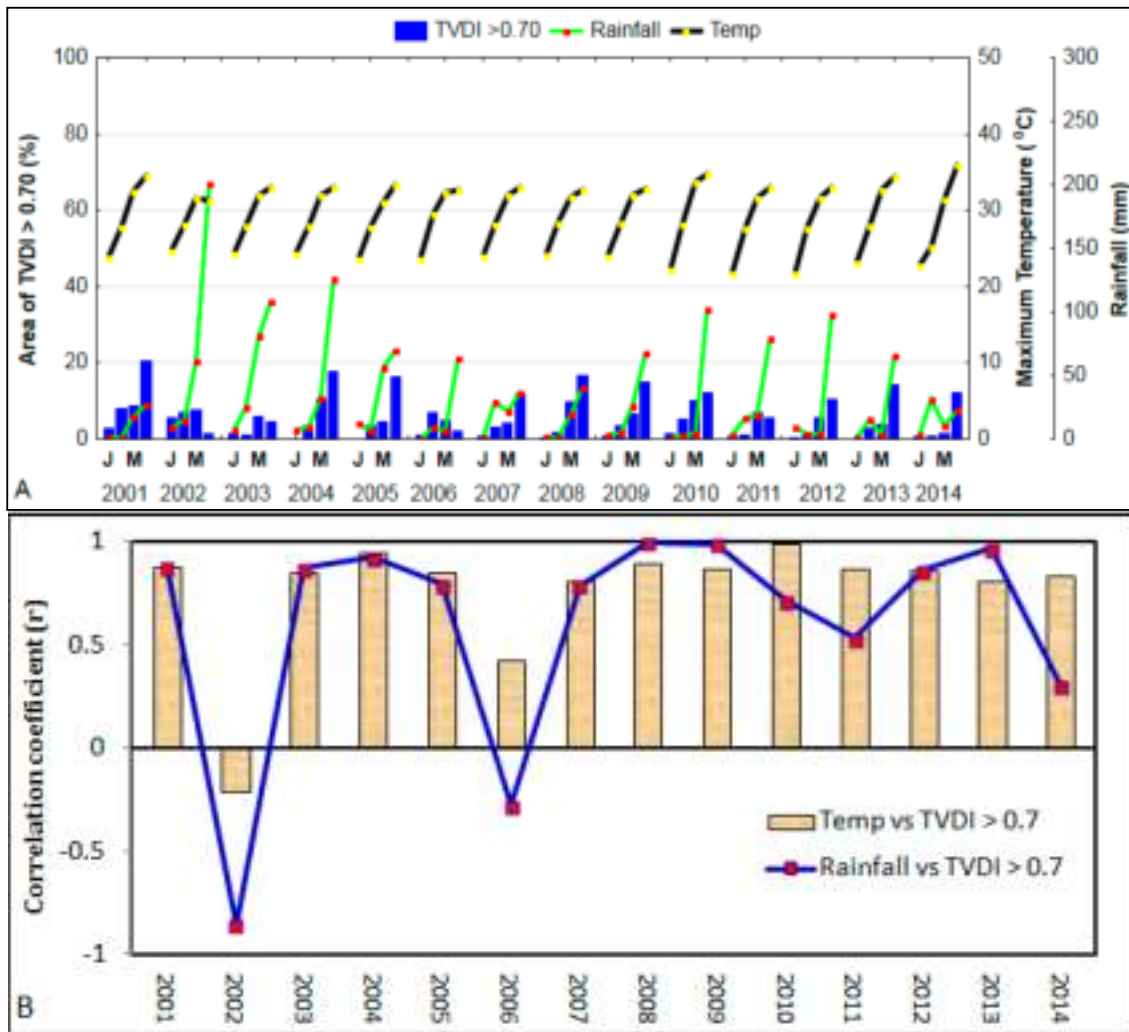


Figure 5. Relationship between highTVDI and temperature and rainfall. (A) is the integrated display of highTVDI area, rainfall and temperature where J indicates January and M indicates March. (B) is the correlation between area of highTVDI and temperature, as well as between highTVDI and rainfall.

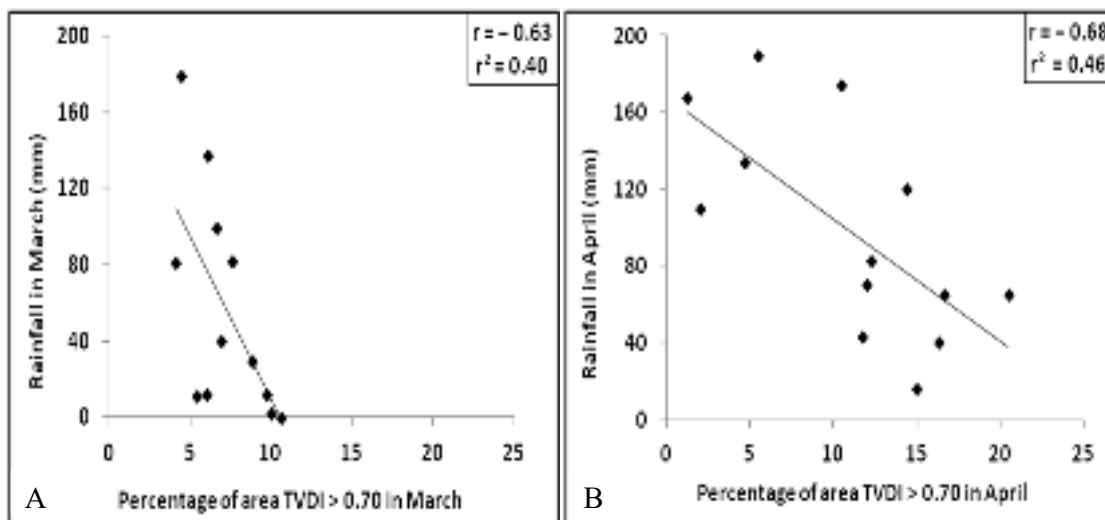


Figure 6. Relationship between highTVDI and rainfall at selected meteorological stations. In graph 6A, we used 12 years of data, and in graph 6B, we used 13 years of data; (A) Percentage of area TVDI > 0.70 in March; (B) Percentage of area TVDI > 0.70 in April.

4.3. TVDI Results and Field Observations

The TVDI results and climate variables suggested that the major factor behind the low TVDI was ground water-based irrigation, with temperature playing a minor role. On the other hand, temperature and rainfall both played major roles in the high TVDI area, with little or no impact from irrigation. To confirm this, it would be necessary to have in situ field data that are unfortunately rarely available in developing countries such as Bangladesh. Therefore, a small-scale field campaign was carried out in the months of March and April to examine the field situation/moisture conditions. Several locations within the (i) low TVDI areas and (ii) high TVDI areas were investigated to determine the real ground conditions.

4.3.1. Field Observations in the Low TVDI Area

In low TVDI areas, 10 sites were visited (Figure 7A–J) to understand the field conditions. Field data clearly revealed that the ground surface was largely covered by green HYV boro rice in different growing stages, namely (i) the booting/heading stage (Figure 7A–C,K) (ii) the flowering and milk stage (Figure 7D,E,L), and (iii) the dough stage (Figure 7H,M). Apart from the boro rice fields, homestead areas with vegetation cover are normally found throughout the investigated area, which can be seen at the edges of every picture (Figure 7B–K).

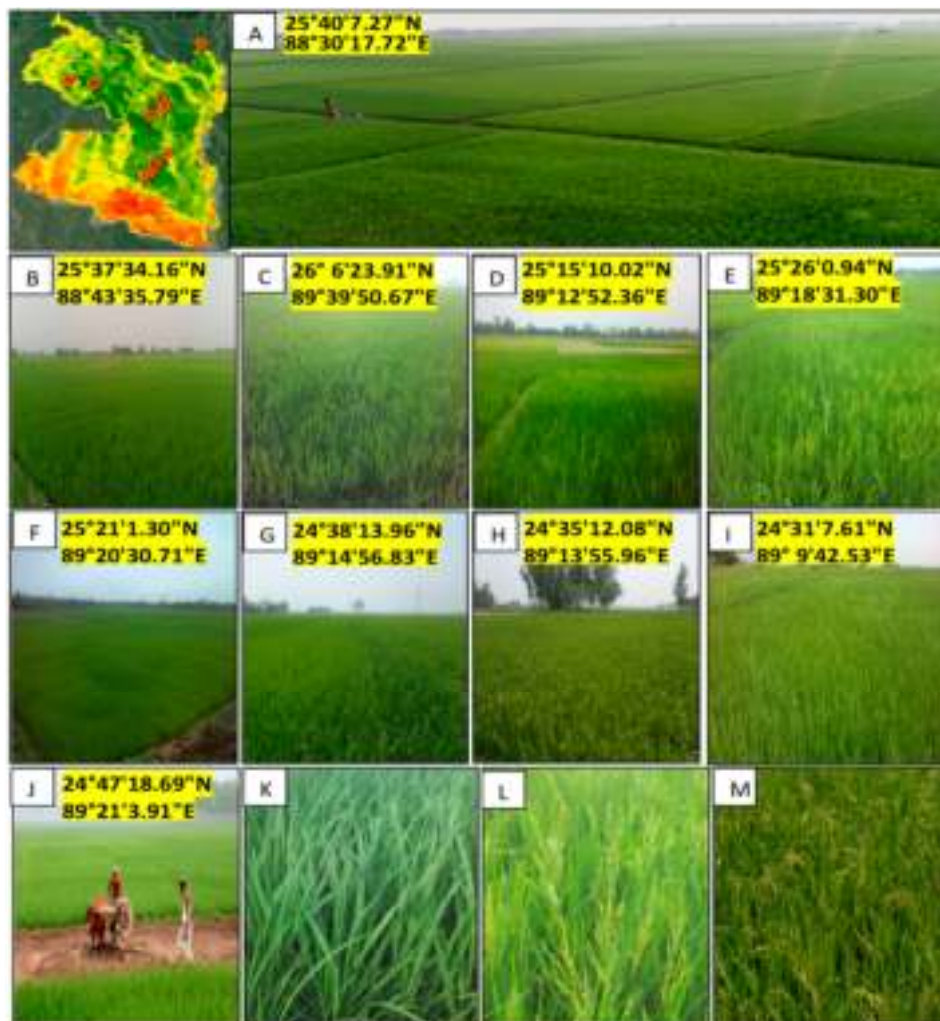


Figure 7. Field observations in low TVDI area. Booting/heading stage (K), flowering and milk stage (L), and dough stage (M).

Besides the overall field conditions, we found that the level of soil moisture was not the same for all irrigated fields (Figure 8). Some fields were completely saturated with stagnant water (Figure 8A,B), while

wet (Figure 8C) and moist (Figure 8D) ground conditions were also observed in some fields. In addition, irrigated fields with different levels of soil moisture deficit were also found (Figure 8E–H). This is probably due to several reasons, such as weeding practices, the temporary mechanical failure of irrigation equipment, negligence, or lack of financial ability to irrigate the fields. However, hardly any fields were found to be completely dry or suffering from severe drought conditions during the field campaign.

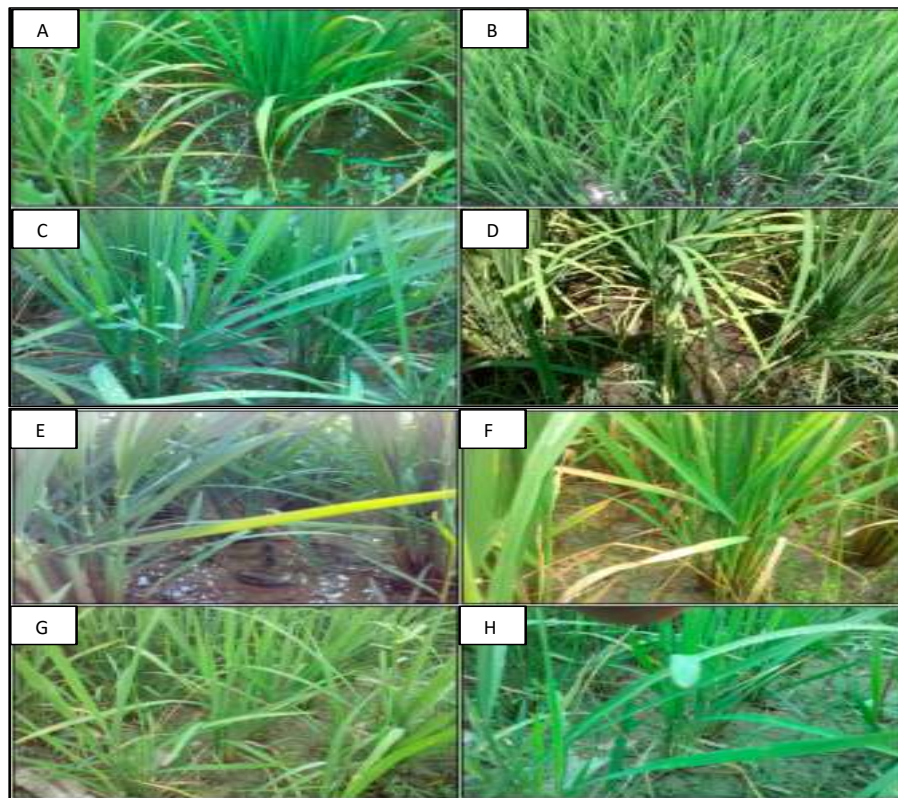


Figure 8. Variation of soil moisture conditions in lowTVDI area. Completely saturated with stagnant water (A,B), wet (C), and moist ground conditions (D). Irrigated fields with different levels of soil moisture deficit (E–H).

The findings listed above indicate that the TVDI results appear to be in good agreement with field conditions. There were no major soil moisture deficits where the $TVDI < 0.70$. Indeed, our results indicate that in the lowTVDI areas, irrigation played a major role in reducing the effect of temperature during the dry season. Furthermore, the field observations suggest that the variation of TVDI values within the lowTVDI area is attributable to several other factors: (i) spatial variation in rainfall, (ii) variation in boro rice planting times, and thus different growing stages of rice, (iii) weeding practices, (v) boro rice fields with other fragmented land use/cover within the 1 km pixel, and (vi) possible small calibration errors associated with the two satellite products.

4.3.2. Field Observations in HighTVDI Areas

The field observations of highTVDI areas were carried out in the two regions where highTVDI areas are concentrated: (i) the High Barind Tract (HBT) and (ii) the Ganges River Floodplain (GRFP).

Field Observations in the HBT HighTVDI Area

Completely different ground conditions were observed in the highTVDI HBT region (Figure 9) compared to the lowTVDI areas (Figure 7). In this region, few green fields were observed, and most land parcels were fallow (Figure 9A1) due to the inadequate soil moisture associated with low rainfall and high temperatures. The severity of dryness can be seen from the cracking of surface soil (Figure 9A2),

although a few days before the field investigation, there was a sudden rainfall event throughout the area, which moistened the soil and caused water logging in low-lying areas (Figure 9B1). In this area, fallow land with dry bare soil was dominant, along with some HYV boro rice where water supply from a deep tube well was available (Figure 9A3,D1). In addition, another type of land cover, i.e., plantations were observed (Figure 9B2,C1,A3).

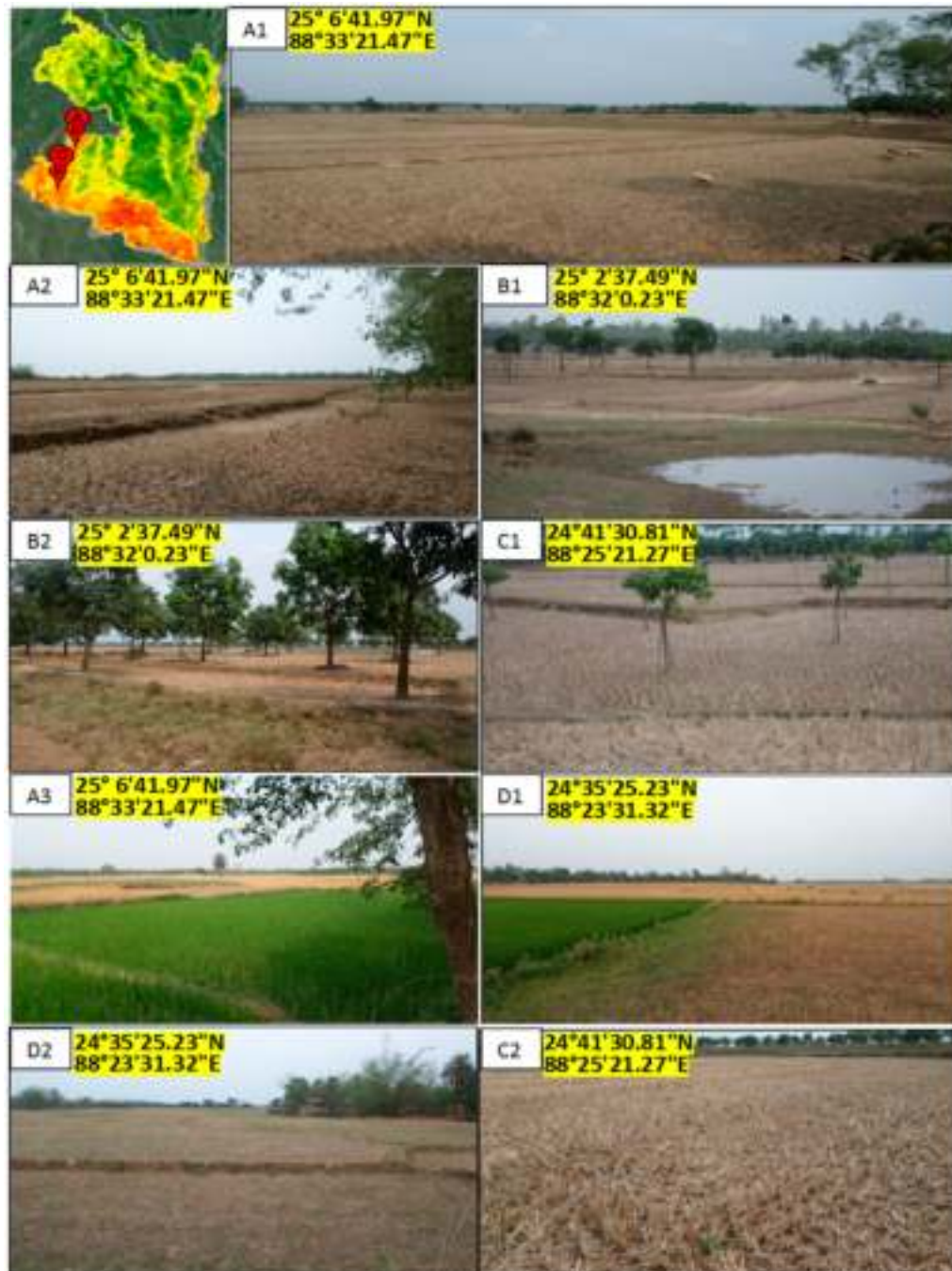


Figure 9. Field observations in high TVDI area in the High Barind Tract (HBT) region.

Field investigation indicates that a higher degree of soil moisture deficit prevails in this region during the late dry season (March and April) than in the low TVDI areas (Figure 7), unless there is water from irrigation or sudden rainfall. This field condition of severe soil moisture deficit or dryness is clearly in agreement with the obtained TVDI results ($\text{TVDI} > 0.70$) and indicates that the TVDI can effectively identify the drought-prone areas. The field observations confirmed that the main

factors behind this dryness are the low rainfall and high temperature. The influence of irrigation can be seen in Figure 9A3,D1, in which some parts of the field are irrigated (no dryness), while others are mostly dry and fallow. However, there is still a variation of TVDI values in the highTVDI area, which is probably attributed due to several minor factors observed during the field investigations, such as (i) different stages of plantation growth (Figure 9B1,B2,C1), (ii) different grazing conditions (Figure 9C2,D2), and (iii) occasional rainfall (Figure 9B1).

Field Observations in the GRFP HighTVDI Area

Several locations were visited during the field campaign in the highTVDI area of GRFP (marked with circles on Figure 10). A large part of the area was fallow after harvesting of the previous crop (Figure 10A), and it was covered by dry wheat straw, as well as different kinds of grass, weeds, small crops, and plantations (Figure 10A–H). Completely empty parcels of ploughed land were also found in many parts of this region (Figure 10I,J). The only significant field crop observed was sugarcane at different stages of growth (Figure 10K–M), which was likely due to its lower water requirement and ability to obtain moisture from deeper soil compared to other crops. Overall, this field campaign found this area to be extremely dry and affected by different degrees of drought severity due to the lack of soil moisture caused by low rainfall and high temperatures.



Figure 10. Field observations in the severe drought (highTVDI) area in the low Ganges River floodplain (GRFP) region.

The observable soil moisture deficit in the GRFP region of the study area is in agreement with the TVDI results, indicating a drought situation based on high TVDI values. Similar to the HBT region, the main factors underlying the severity of drought were the high temperatures and low rainfall in the absence of irrigation moisture. Indeed, there are several other factors such as plantations, cropping patterns, land use/cover, underground soil moisture, top soil conditions, etc., that play minor roles in the variation in drought conditions, resulting in the spatial and temporal variation in the TVDI results.

5. Discussion

This study investigated the future risk of drought across the northwestern part of Bangladesh by integrating remote sensing-based drought indices with climate variables and field observations. The results indicate that the remote sensing-based drought index, the TVDI, is very effective for identifying drought, as the TVDI results are comparable with and confirmed by field observations from both irrigated and non-irrigated surfaces. Our findings on the effectiveness of the TVDI agree with other studies that report that NDVI-LST-based drought indices; especially, the TVDI are effective for the investigation of soil moisture conditions across a range of land features and agro-ecological zones [21,49,50,55].

In addition to the effectiveness of the remote sensing-based drought index TVDI, we investigated the integrated use of the TVDI with the climate variables of temperature and rainfall by grouping the TVDI results into two groups: i.e., low TVDI and high TVDI. In low TVDI areas, we found a very large disagreement between the TVDI results and climate variables. For example, there are many areas where temperature is high and rainfall is low, but the TVDI result indicates no moisture deficit, even in the month of April (hottest month), and this is due to intensive irrigation practices. The field observations in low TVDI areas confirm the TVDI results but do not correspond to the observed temperature and rainfall conditions. In contrast, we found that the TVDI results are in complete agreement with temperature and rainfall in high TVDI areas that are characterized by high temperature, low rainfall, and a lack of irrigation practices. Field observations from the high TVDI regions represent the TVDI outcomes and observable temperature and rainfall reasonably well. The TVDI results and climate variables suggest that the major factor behind the large low TVDI area is groundwater-based irrigation, while temperature played a minor role. On the other hand, temperature and rainfall both played major roles in the high TVDI area, while irrigation had little or no impact.

The successful integrated use of TVDI, climate variables, and field observations in high TVDI areas indicate that this integration can effectively be used for the detection of the spatial and temporal variation in drought over the study area. However, the massive seasonal (Figure 4a) long-term (Figure 11) anomalies between low TVDI areas and climate variables provided us with an indirect opportunity to understand/detect the potential risks of drought in this complex environmental setting where the low TVDI and field observations tell us that there is no deficit of soil moisture due to intensive irrigation.

We observed from Figure 11 that over the 14-year period, the average temperature is high ($>32^{\circ}\text{C}$) and the average rainfall is low ($<35\text{ mm/month}$), especially in the months of March and April, but 80% of the areas showed low TVDI values. The percentage of low TVDI areas (Figure 11) indicated the actual ground conditions detected by the remote sensing-based TVDI index, and the field observations agreed with the TVDI outcomes. The indicated high temperature and low rainfall (Figure 11) over the period would be expected to instigate meteorological drought as well as agricultural drought, and this is indeed observed in high TVDI regions, but not in the low TVDI regions due to intensive irrigation.

Results suggest that the integrated use of the remote sensing-based TVDI index (which reveals ground conditions) and climate variables (which reveal climatic conditions), along with field observations (which provide in situ evidence), can reliably indicate the present state and future risk of drought in complex environmental settings. However, despite the current absence of agricultural drought, Figure 11 clearly shows that meteorological drought exists in this region but did not trigger agricultural drought due to intensive irrigation by groundwater. Therefore, the future risk of severe agricultural drought

cannot be neglected, since the current droughtless condition is completely dependent on anthropogenic factors (i.e., groundwater supply) rather than natural factors (i.e., rainfall and temperature).

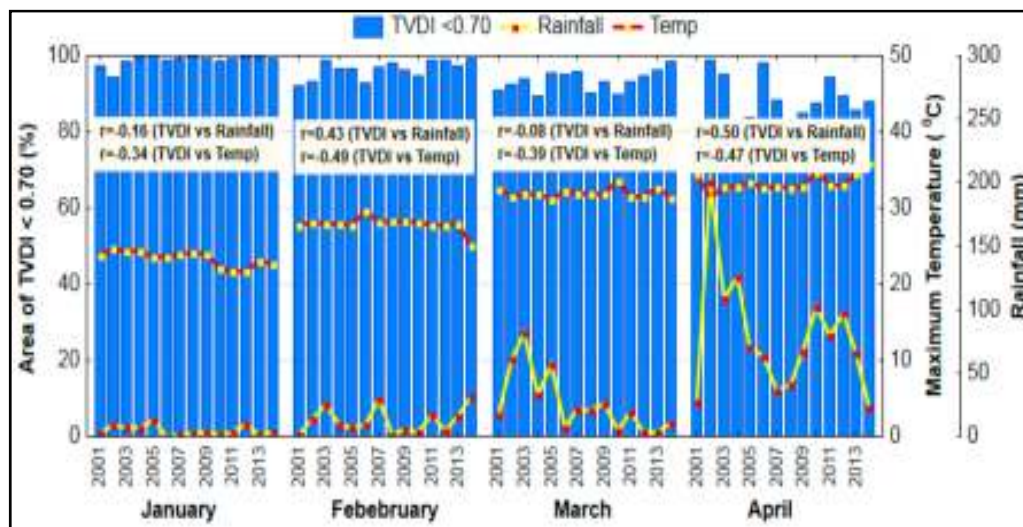


Figure 11. Long-term relationship between low TVDI and climate variables (temperature and rainfall).

Nevertheless, the future drought risk factor can be explained by the fact that in the past, several notable severe drought incidents were observed during this season in NWB due to low rainfall and high temperature. However, the drought scenario began to change after the introduction of irrigation activity in the mid-1980s, when the groundwater began to be used as a major source of water supply for rice cultivation [36,56].

It is obvious that at present, the groundwater based-irrigation systems, in NWB and throughout Bangladesh, not only significantly reduced the severity of drought, especially in the pre-monsoon season, but also helped meet the increasing food demands of the rapidly growing population in Bangladesh [12,56,57]. However, there is a growing concern that the groundwater table in NWB as well as the other parts in Bangladesh is gradually declining in an unsustainable manner due to large abstraction by the irrigation projects [58–60]. Prior to the widespread abstraction of groundwater for irrigation, water tables in the mostly unconfined aquifers of Bangladesh were generally shallow with a weak seasonal fluctuating trend [56].

Study [12] indicated that the groundwater table had a declining trend over the last 30 years (1981–2011), which implies that groundwater use is not sustainable in NWB and found that the magnitude of the decline in the groundwater table has been between -2.3 and -11.5 m during the pre-monsoon period. Studies indicated that this gradual declination is mainly due to the over exploitation of groundwater rather than recharging the aquifer, since about 95% of irrigation water for Boro rice cultivation comes from groundwater, which is extracted mainly by shallow tubewells (STW) and deep tubewells (DTW) [56,61]. Moreover, [12] pointed out that in NWB, the most severely depleted areas are Rajshahi followed by Pabna, Bogra, Dinajpur, and Rangpur.

Therefore, considering the finding of this study that “there is meteorological drought in NWB” and the finding from existing literature [12,56,59,60] that the “underground water table is declining in an unsustainable manner due to large abstraction for irrigation”, it is highly likely that there will be an imbalance between the availability of underground water and requirement for irrigation. The probable scarcity of underground water in the future may transform the existing meteorological drought into severe agricultural drought, which is at present is observable in only a small part of the study area (NWB). As a result, we could say that there is a risk of drought in NWB as well as in Bangladesh if adequate measures are not going to be taken in advance to prevent the unwanted decline of underground water.

6. Conclusions

In this study, a simple approach for detecting drought and its potential risk in NWB is presented. Several statistical and causal relationships were utilized to compare the TVDI results with the climate variables (temperature and rainfall) and with field observations. Although Bangladesh has undergone several severe droughts in the past, massive irrigation practices have greatly changed the occurrence of severe drought in recent years. Therefore, at present, we can only easily observe meteorological drought, especially in the months of March and April. However, agricultural drought is observable in only a small part of the study area (NWB) at present, and it does not occur over the larger part of NWB, as the effect of meteorological drought is compensated by underground water-based irrigation.

However, the concern over the falling underground water table undoubtedly poses a potential risk of drought since not only the volume of underground water availability but also the exact amount of use of underground water are not well known. Moreover, the overwhelming population, food insecurity, and poor water management put unprecedented pressure on the groundwater, resulting in the gradual decline of the water level. Unfortunately, most of the farmers are still unaware of this situation, and no appropriate measures have been taken yet by the individual or respective authorities to minimize the risk of future underground water supply disruption. This implies that there is still a potential risk of drought in Bangladesh, and any disruption of the underground water supply for irrigation could trigger severe agricultural drought, with catastrophic impacts on food production in this densely populated country.

There were a few limitations of the integrated drought monitoring methodology presented in this study. These include, particularly, the limited amount of satellite data (from 2001–2014), the small number of field observations, as well as slight errors in the satellite product, which are inherent in long-term data processing. Despite these limitations, the study has achieved its objective of illustrating the current state and future risk of drought in this agriculture-based country. Further studies may need to incorporate remote sensing, climate data, and field observations to comprehend drought conditions not only in northwestern part of Bangladesh but also in a regional context. Indeed, there is a trend of rising temperatures and drought incidence in the south Asian region due to climate change, which is illustrated by the very recent severe drought in India.

Supplementary Materials: The following are available online at <http://www.mdpi.com/2072-4292/12/17/2686/s1>.

Author Contributions: M.L.R.S., S.S., B.B.A., and E.S. conceptualized the idea of the research. M.L.R.S. and S.A.M. completed the data processing. M.L.R.S. completed the analysis and writing of the first draft. B.B.A., S.S., E.-S.C., J.S.R. reviewed and updated the first draft. N.J. and M.L.R.S. completed the subsequent editing and prepared the final version of the manuscript. M.L.R.S. and E.S. secured the funding. All authors have read and agreed to the published version of the manuscript.

Funding: This research is supported by the Asia–Pacific Network for Global Change Research (APN, CAF2017-RR02-CMY-Siswanto) project.

Acknowledgments: We thank several colleagues especially Tofiqul Islam, Shingra College, Nator, Rajshahi, Mst. Sadiya Afrin, Agriculture Office, Dinajpur, Emranul Islam, Dept of Geography & Environmental Studies, RU, Bangladesh for their hard work for collecting field data during very hot weather.

Conflicts of Interest: The authors declare no conflict of interest.

References

1. Wilhite, D.A. Drought as a natural hazard: Concepts and definitions. In *Drought: A Global Assessment*; Routledge: London, UK, 2000.
2. Keshavarz, M.R.; Vazifedoust, M.; Alizadeh, A. Drought monitoring using a Soil Wetness Deficit Index (SWDI) derived from MODIS satellite data. *Agric Water Manag.* **2014**, *132*, 37–45. [[CrossRef](#)]
3. Wang, Q.; Wu, J.; Lei, T.; He, B.; Wu, Z.; Liu, M.; Liu, D. Temporal-spatial characteristics of severe drought events and their impact on agriculture on a global scale. *Quart. Int.* **2014**, *349*, 10–21. [[CrossRef](#)]
4. Riebsame, W.; Changon, S.; Karl, T. *Drought and Natural Resources Management in the United States: Impacts and Implications of the 1987-89 Drought*; Westview Press Inc.: Boulder, CO, USA, 1991.

5. IPCC. *Managing the Risks of Extreme Events and Disasters to Advance Climate Change Adaptation; A Special Report of Working Groups I and II of the Intergovernmental Panel on Climate*; Cambridge University Press: Cambridge, UK; New York, NY, USA, 2012; 582p.
6. Kogan, F.; Adamenko, T.; Guo, W. Global and regional drought dynamics in the climate warming era. *Remote Sens Lett.* **2013**, *4*, 364–372. [[CrossRef](#)]
7. Bandyopadhyay, N.; Bhuiyan, C.; Saha, A.K. Heat waves, temperature extremes and their impacts on monsoon rainfall and meteorological drought in Gujarat, India. *Nat. Hazards* **2016**, *82*, 367–388. [[CrossRef](#)]
8. Helmer, M.; Hilhorst, D. Natural disasters and climate change. *Disasters* **2006**, *30*, 1–4. [[CrossRef](#)]
9. Li, Y.; Ye, W.; Wang, M.; Yan, X. Climate change and drought: A risk assessment of crop-yield impacts. *Clim. Res.* **2009**, *39*, 31–46. [[CrossRef](#)]
10. Dahal, P.; Shrestha, N.S.; Shrestha, M.L. Drought risk assessment in central Nepal: Temporal and spatial analysis. *Nat. Hazards* **2016**, *80*, 1913–1932. [[CrossRef](#)]
11. Miyan, M.A. Droughts in asian least developed countries: Vulnerability and sustainability. *Weather Clim. Extrem.* **2015**, *7*, 8–23. [[CrossRef](#)]
12. Dey, N.C.; Bala, S.K.; Islam, A.K.M.S.; Rashid, M.A.; Hossain, M. *Sustainability of Groundwater Use for Irrigation in Northwest Bangladesh*; National Food Policy Capacity Strengthening Programme (NFPCSP): Dhaka, Bangladesh, 2013.
13. Sahoo, R.N.; Dutta, D.; Khanna, M.; Kumar, N.; Bandyopadhyay, S.K. Drought assessment in the Dhar and Mewat Districts of India using meteorological, hydrological and remote-sensing derived indices. *Nat. Hazards* **2015**, *77*, 733–751. [[CrossRef](#)]
14. Thavornnam, W.; Tantemsapya, N.; Armstrong, L. A combination of meteorological and satellite-based drought indices in a better drought assessment and forecasting in Northeast Thailand. *Nat. Hazards* **2015**, *77*, 1453–1474. [[CrossRef](#)]
15. Mishra, A.K.; Singh, V.P. A review of drought concepts. *J. Hydrol.* **2010**, *391*, 202–216. [[CrossRef](#)]
16. Xia, L.; Zhao, F.; Mao, K.B.; Yuan, Z.J.; Zuo, Z.Y.; Xu, T.R. SPI-based analyses of drought changes over the past 60 years in China's major crop-growing areas. *Remote Sens.* **2018**, *10*, 171. [[CrossRef](#)]
17. McKee, T.B.; Doesken, N.J.; Kleist, J. The relationship of drought frequency and duration to time scales. Preprints. In Proceedings of the 8th Conference on Applied Climatology, Anaheim, CA, USA, 17–22 January 1993.
18. Palmer, W.C. *Meteorological Drought*; U.S. Weather Bureau: Washington, DC, USA, 1965; pp. 45–58.
19. Rouse, J.W.; Haas, R.H.; Schell, J.A.; Deering, D.W. Monitoring Vegetation Systems in the Great Okains with ERTS. *Third Earth Resour. Technol. Satell. Symp.* **1973**, *1*, 325–333.
20. Kogan, F.N. Application of vegetation index and brightness temperature for drought detection. *Adv. Sp. Res.* **1995**, *15*, 91–100. [[CrossRef](#)]
21. Sandholt, I.; Rasmussen, K.; Andersen, J. A simple interpretation of the surface temperature/vegetation index space for assessment of surface moisture status. *Remote Sens. Environ.* **2002**, *79*, 213–224. [[CrossRef](#)]
22. Son, N.T.; Chen, C.F.; Chen, C.R.; Chang, L.Y.; Minh, V.Q. Monitoring agricultural drought in the Lower Mekong Basin using MODIS NDVI and land surface temperature data. *Int. J. Appl. Earth Obs. Geoinf.* **2012**, *18*, 417–427. [[CrossRef](#)]
23. Yoon, D.-H.; Nam, W.-H.; Lee, H.-J.; Hong, E.-M.; Feng, S.; Wardlow, B.D.; Tadesse, T.; Svoboda, M.D.; Hayes, M.J.; Kim, D.-E. Agricultural Drought Assessment in East Asia Using Satellite-Based Indices. *Remote Sens.* **2020**, *12*, 444. [[CrossRef](#)]
24. Brown, J.F.; Wardlow, B.D.; Tadesse, T.; Hayes, M.J.; Reed, B.C. The Vegetation Drought Response Index (VegDRI): A New Integrated Approach for Monitoring Drought Stress in Vegetation. *GIScience Remote Sens.* **2008**, *45*, 16–46. [[CrossRef](#)]
25. Jerrod, L.; Sweeney, A.; Ceccato, P. An agricultural drought severity index using quasi-climatological anomalies of remotely sensed data. *Int. J. Remote Sens.* **2016**, *37*, 913–925.
26. Tigkas, D.; Vangelis, H.; Tsakiris, G. An enhanced effective Reconnaissance drought index for the characterisation of agricultural drought. *Environ. Process.* **2017**, *4*, 1–12. [[CrossRef](#)]
27. Tran, T.V.; Tran, D.X.; Myint, S.W.; Latorre-Carmona, P.; Ho, D.D.; Tran, P.H.; Dao, H.N. Assessing Spatiotemporal Drought Dynamics and Its Related Environmental Issues in the Mekong River Delta. *Remote Sens.* **2019**, *11*, 2742. [[CrossRef](#)]

28. Gao, Z.; Gao, W.; Chang, N.B. Integrating temperature vegetation dryness index (TVDI) and regional water stress index (RWSI) for drought assessment with the aid of LANDSAT TM/ETM+ images. *Int. J. Appl. Earth Obs. Geoinf.* **2011**, *13*, 495–503. [[CrossRef](#)]
29. Du, L.; Tian, Q.; Yu, T.; Meng, Q.; Jancso, T.; Udvardy, P.; Huang, Y. A comprehensive drought monitoring method integrating MODIS and TRMM data. *Int. J. Appl. Earth Obs. Geoinf.* **2013**, *23*, 245–253. [[CrossRef](#)]
30. Han, Y.; Li, Z.; Huang, C.; Zhou, Y.; Zong, S.; Hao, T.; Niu, H.; Yao, H. Monitoring Droughts in the Greater Changbai Mountains Using Multiple Remote Sensing-Based Drought Indices. *Remote Sens.* **2020**, *12*, 530. [[CrossRef](#)]
31. Gebrehiwot, T.; van der Veen, A.; Maathuis, B. Spatial and temporal assessment of drought in the northern highlands of Ethiopia. *Int. J. Appl. Earth Obs. Geoinf.* **2011**, *13*, 309–321. [[CrossRef](#)]
32. Goetz, S.J. Multi-sensor analysis of NDVI, surface temperature and biophysical variables at a mixed grassland site. *Int. J. Remote Sens.* **1997**, *18*, 71–94. [[CrossRef](#)]
33. Rhee, J.; Im, J.; Carbone, G.J. Monitoring agricultural drought for arid and humid regions using multi-sensor remote sensing data. *Remote Sens. Environ.* **2010**, *114*, 2875–2887. [[CrossRef](#)]
34. Meng, L.; Dong, T.; Wen, Z. Drought monitoring using an Integrated Drought Condition Index (IDCI) derived from multi-sensor remote sensing data. *Nat. Hazards* **2016**, *80*, 1135–1152. [[CrossRef](#)]
35. Brammer, H. Drought in Bangladesh: Lessons for planners and administrators. *Disasters* **1987**, *11*, 21–29. [[CrossRef](#)]
36. Paul, B.K. Coping mechanisms practised by drought victims (1994/5) in North Bengal, Bangladesh. *Appl. Geogr.* **1998**, *18*, 355–373. [[CrossRef](#)]
37. Shahid, S. Spatial and temporal characteristics of droughts in the western part of Bangladesh. *Hydrol. Process.* **2008**, *22*, 2235–2247. [[CrossRef](#)]
38. Habiba, U.; Shaw, R.; Takeuchi, Y. Drought risk reduction through a Socio-economic, Institutional and Physical approach in the northwestern region of Bangladesh. *Environ. Hazards* **2011**, *10*, 121–138. [[CrossRef](#)]
39. Rashid, H.E. *Geography of Bangladesh*, 2nd ed.; University Press Ltd.: Dhaka, Bangladesh, 1991; pp. 5–75.
40. Shahid, S. Impacts of Climate Change on Irrigation Water Demand in Northwestern Bangladesh. *Climatic Chang.* **2011**, *105*, 433–453. [[CrossRef](#)]
41. Wahid, S.M.; Babel, M.S.; Gupta, A.D.; Clemente, R.S. Spatial assessment of groundwater use potential for irrigation in Teesta Barrage Project in Bangladesh. *Hydrogeol. J.* **2007**, *15*, 365–382. [[CrossRef](#)]
42. BBS (Bangladesh Bureau of Statistics). 2015 Estimates of Boro Rice (Husked), 2013–2014. Government of the People’s Republic of Bangladesh: Dhaka, Bangladesh. Available online: <http://203.112.218.65:8008/WebTestApplication/userfiles/Image/Agriculture/Boro-2013-14.pdf> (accessed on 1 September 2016).
43. Tucker, C.J.; Choudhury, B.J. Satellite remote sensing of drought conditions. *Remote Sens. Environ.* **1987**, *23*, 243–251. [[CrossRef](#)]
44. Ji, L.; Peters, A.J. Assessing vegetation response to drought in the northern Great Plains using vegetation and drought indices. *Remote Sens. Environ.* **2003**, *87*, 85–98. [[CrossRef](#)]
45. Ghulam, A.; Qin, Q.; Teyip, T.; Li, Z.L. Modified perpendicular drought index (MPDI): A real-time drought monitoring method. *ISPRS J. Photogramm. Remote Sens.* **2007**, *62*, 150–164. [[CrossRef](#)]
46. Moran, M.S.; Clarke, T.R.; Inoue, Y.; Vidal, A. Estimating crop water deficit using the relation between surface–air temperature and spectral vegetation index. *Remote Sens. Environ.* **1994**, *49*, 246–263. [[CrossRef](#)]
47. Lambin, E.F.; Ehrlich, D. The surface temperature-vegetation index space for land cover and land-cover change analysis. *Int. J. Remote Sens.* **1996**, *17*, 463–487. [[CrossRef](#)]
48. Owen, T.W.; Carlson, T.N.; Gillies, R.R. An assessment of satellite remotely-sensed land cover parameters in quantitatively describing the climatic effect of urbanization. *Int. J. Remote Sens.* **1998**, *19*, 1663–1681. [[CrossRef](#)]
49. Wan, Z.M.; Wang, P.X.; Li, X.W. Using MODIS land surface temperature and normalized difference vegetation index products for monitoring drought in the southern Great Plains, USA. *Int. J. Remote Sens.* **2004**, *25*, 61–72. [[CrossRef](#)]
50. Chen, C.F.; Son, N.T.; Chang, L.Y.; Chen, C.C. Monitoring of soil moisture variability in relation to rice cropping systems in the Vietnamese Mekong Delta using MODIS data. *Appl. Geogr.* **2011**, *31*, 463–475. [[CrossRef](#)]
51. Dhorde, A.G.; Patel, N.R. Spatio-temporal variation in terminal drought over western India using dryness index derived from long-term MODIS data. *Ecol. Inform.* **2016**, *32*, 28–38. [[CrossRef](#)]

52. Patel, N.R.; Anapashsha, R.; Kumar, S. Assessing potential of MODIS derived temperature/vegetation condition index (TVDI) to infer soil moisture status. *Int. J. Remote Sens.* **2009**, *9*, 23–39. [[CrossRef](#)]
53. Shahid, S.; Behrawan, H. Drought risk assessment in the western part of Bangladesh. *Nat. Hazards* **2008**, *46*, 391–413. [[CrossRef](#)]
54. Dash, B.K.; Rafiuddin, M.; Khanam, F. Characteristics of meteorological drought in Bangladesh. *Nat. Hazards* **2012**, *64*, 1461–1474. [[CrossRef](#)]
55. FAO. *AQUASTAT Country Profile of Bangladesh*, version 2010; FAO: Rome, Italy, 2011.
56. Mojid, M.A.; Parvez, M.F.; Mainuddin, M.; Hodgson, G. Water table trend—A sustainability status of groundwater development in North-West Bangladesh. *Water* **2019**, *11*, 1182. [[CrossRef](#)]
57. Ingram, J.S.I. From Food Production to Food Security: Developing Interdisciplinary, Regional-Level Research. Ph.D. Thesis, Wageningen University, Wageningen, The Netherlands, 2011. Available online: <https://edepot.wur.nl/176450> (accessed on 5 March 2019).
58. Hoque, M.A.; Hoque, M.M.; Ahmed, K.M. Declining groundwater level and aquifer dewatering in Dhaka metropolitan area, Bangladesh: Causes and quantification. *Hydrogeol. J.* **2007**, *15*, 1523–1534. [[CrossRef](#)]
59. Kirby, J.M.; Ahmada, M.D.; Mainuddina, M.; Palashb, W.; Quadirc, M.E.; Shah-Newazc, S.M.; Hossain, M.M. The impact of irrigation development on regional groundwater resources in Bangladesh. *Agric. Water Manag.* **2015**, *159*, 264–276. [[CrossRef](#)]
60. Mollah, A.H. Groundwater Level Declination in Bangladesh: System Dynamics Approach to Solve Irrigation Water Demand During Boro Season. Master's Thesis, University of Bergen, Bergen, Norway, 2017. Available online: <https://pdfs.semanticscholar.org/32c5/36bcd341e6110376c602e6133eda3ef87d7f.pdf> (accessed on 15 May 2019).
61. Mainuddin, M.; Rawson, H.M.; Poulton, P.L.; Ali, R.; Roth, C.; Islam, K.M.; Saifuzzaman, M.; Rahman, M.M.; Quader, M.E.; Shah-Newaz, S.M. *Scoping Study to Assess Constraints and Opportunities for Future Research into Intensification of Cropping Systems in Southern Bangladesh*; ACIAR Report; ACIAR: Canberra, Australia, 2013.



© 2020 by the authors. Licensee MDPI, Basel, Switzerland. This article is an open access article distributed under the terms and conditions of the Creative Commons Attribution (CC BY) license (<http://creativecommons.org/licenses/by/4.0/>).